ELSEVIER

Polymer 42 (2001) 137–142

polymer

www.elsevier.nl/locate/polymer

Study of gelation kinetics and gel structure for *trans*-decalin solutions of isotactic polystyrene using ultrasonic measurements

A. Tanaka[a,*], K. Kago[b], Y. Uchida[b], H. Nagata[b], Koh-hei Nitta[c]

[a]*Department of Materials Science, The University of Shiga Prefecture, Hikone 522-8533, Japan*
[b]*Department of Polymer Chemistry, Kyoto University, Kyoto 606-8317, Japan*
[c]*School of Materials Science, JAIST, Ishikawa 923-1292, Japan*

Received 22 September 1999; received in revised form 26 April 2000; accepted 26 April 2000

Abstract

The gelation mechanism was investigated using in situ ultrasonic measurements. It was found that the gelation takes place by different mechanisms, depending upon quenching temperature. When iPS/*trans*-decalin solution was allowed to quench above the coexistence curve, the gelation was caused by crystallization. On the other hand, when it was allowed to quench below the coexistence curve, the gelation was caused mainly by liquid–liquid phase separation. Therefore, the junction point structure may be crystallite for the former gels, while for the latter ones, it may be a solvated structure. This conclusion was also supported by other measurements such as IR and NMR spectra, as well as by visual and tactual observations.

Keywords: Physical gels; Isotactic polystyrene; Liquid–liquid phase separation

1. Introduction

Various kinds of polymers are known to form thermoreversible gels in different solvents. Accordingly, a large number of gelation mechanisms have been proposed in the literature. In addition, for isotactic polystyrene (iPS) thermoreversible gels, various types of junction point structures have been proposed for the gels prepared using various solvents [1–18]. Here, we will briefly review on the gelation mechanism for a particular solvent system: iPS and decalin. Previously, for iPS/decalin gels, crystallites consisting of 3_1 helix, which is generally observed upon crystallization either from the bulk or from the dilute solutions [1], were considered the junction point structure. However, Keller and coworkers [2] showed that a different form of crystallites, 12_1 helix acts as a junction point. This proposal is based on the observation by X-ray diffraction for the gels partially dried and stretched, that is, on a reflection at 0.51 nm that is attributed to diffraction from the 006 plane. This form was supported by Sundararajan et al. [6]. They considered that solvent molecules stabilize the 12_1 helix, that is, solvated crystal is formed. Guenet et al. disproved the 12_1 helix structure by means of neutron diffraction experiments [8,10], and proposed to a structure (ladderlike model) closer to a nematic liquid-crystalline state than to a crystalline state [11–16]. However, the helix solvation has been questioned based on NMR experiments by Perez et al. [12]. Moreover, it has been reported by Guenet and coworkers [18] that only two kinds of molecular aggregation states were observed for iPS/*trans*-decalin gels: smectic liquid-crystalline and crystalline states. While, for iPS/*cis*-decalin gels, three kinds of molecular aggregation states were observed: nematic liquid-crystalline, smectic liquid-crystalline and crystalline states.

Thus, for the iPS/decalin system, either of crystallization, liquid–liquid phase separation, or vitrification is considered as a cause of thermal gelation. However, a question remains: by what sort of preparation is a particular junction point structure formed? It seems that in most cases no care has been taken in the preparation condition of gels, such as cooling temperature and cooling rate. That is, there has been little attempt to correlate kinetic data with the gelation mechanisms.

In this study, the gelation kinetics of the iPS/*trans*-decalin system was investigated using ultrasonic measurements. Then, the effect of the gelation kinetics on gel structure was discussed. It should be noted that ultrasonic quantities are very sensitive to the change in molecular aggregation such as phase transition.

* Corresponding author. Tel.: +81-749-28-8358; fax: +81-749-28-8583.
E-mail address: tanaka@mat.usp.ac.jp (A. Tanaka).

0032-3861/01/$ - see front matter
PII: S0032-3861(00)00344-X

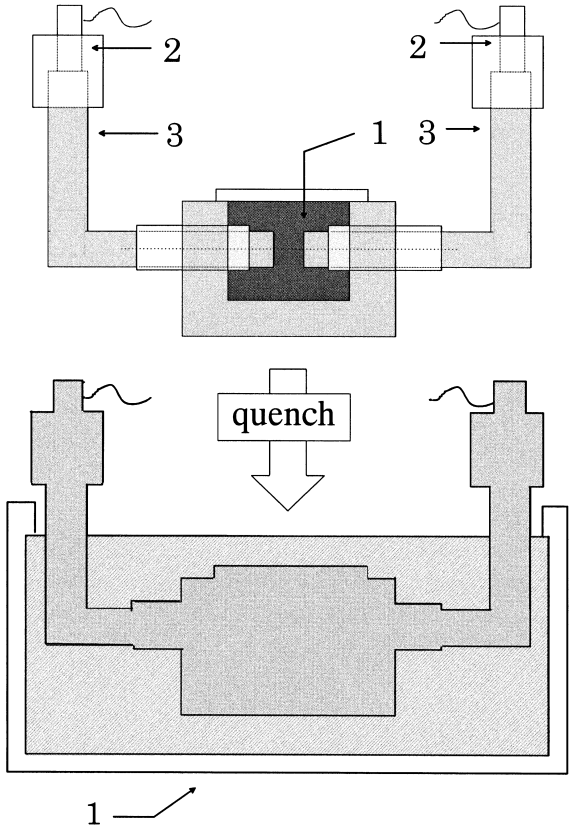

Fig. 1. Schematic diagram of the cell for ultrasonic *T*-drop measurements.

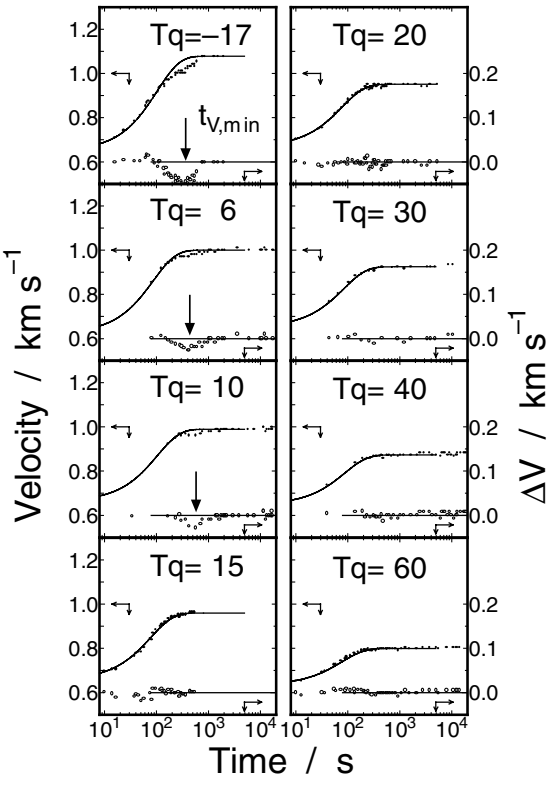

Fig. 2. The variation of the ultrasonic velocity with time for 10 wt% iPS/*trans*-decalin solution when the solution was allowed to quench into various temperatures (T_q). The closed circles denote the velocity. The curves were fit by Eq. (3). The open circles denote a deviation of the velocity from the fitting curve. The arrow indicates the time, t_{vmin} at which the velocity was minimum.

2. Experimental section

2.1. Materials

The iPS samples were supplied from Idemitsu Petrochemical Co. Ltd. The isotacticity of the samples was over 97%. The number and weight average molecular weights were 5.73×10^5 and 2.20×10^6, respectively. *Trans*-decalin of high-purity grade (above 99%) was purchased from Tokyo–Kasei Co. Ltd, and was employed without further purification.

2.2. Experimental procedure and ultrasonic measurements

A mixture of polymer (iPS) and solvent (*trans*-decalin) with the desired ratios was heated to a sufficiently high temperature to allow the polymer to dissolve. Then, *trans*-decalin solutions of iPS (described as iPS/*trans*-decalin, hereafter) with various concentrations (5, 10 and 15 wt%) were prepared. The solution was poured into a cell, schematically illustrated in Fig. 1. The solution in the cell was kept at 150°C for a few minutes, and then the cell was plunged into a cooling-bath, which was preset at various temperatures between −30 and 60°C. Ultrasonic velocity and ultrasonic intensity were measured as a function of time after immersion into the cooling-bath.

The ultrasonic velocity,*v* and the attenuation coefficient, α was determined in the same way as described in the previous paper [19] using the following equations, respectively:

$$v = L/\Delta t \tag{1}$$

and

$$\alpha = \frac{1}{L}\ln(A_0/A) \tag{2}$$

where L and Δt are the traveling distance and the traveling time of ultrasonic wave in the sample, respectively. A and A_0 are the amplitude of ultrasonic wave at a traveling distance of L and zero, respectively.

3. Results and discussion

For iPS/*trans*-decalin solutions with concentrations of 5, 10 and 15 wt%, the ultrasonic velocity was measured as a function of time after immersion into a cooling-bath held at various temperatures between −25 and 60°C. Fig. 2 shows the variation of the velocity with time for 10 wt% iPS/*trans*-decalin solution when the solution was allowed to quench into different temperatures. In the figures, closed circles

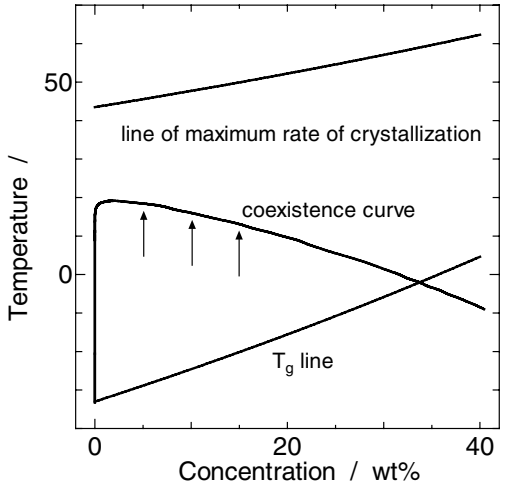

Fig. 3. The coexistence curve on the temperature–concentration phase diagram, the glass transition line and the line of maximum crystallization.

denote the ultrasonic velocity. As is seen in the figure, the velocity increased rather monotonically with time. The monotonous increase must be due to the decrease in temperature of the solution, that is, the increase in the ratio of the bulk modulus to the density for the solution. Thus, if there are no molecular aggregation state changes, the velocity must be characterized by the first-order equation,

$$v = v_q + (v_0 - v_q)\exp(-kt) \tag{3}$$

where v is the velocity at time t, v_0, the velocity of the solution prior to quenching, that is, the velocity at 150°C; v_q, the velocity of the solution at times passed long enough after quenching, that is, the velocity at the quenching temperature; and k, the rate constant. The parameters, v_0, v_q and k were selected in such a way that velocity data are put on the curve expressed as in Eq. (3), as much as possible. The curve thus obtained seems to fit quite well with the data,

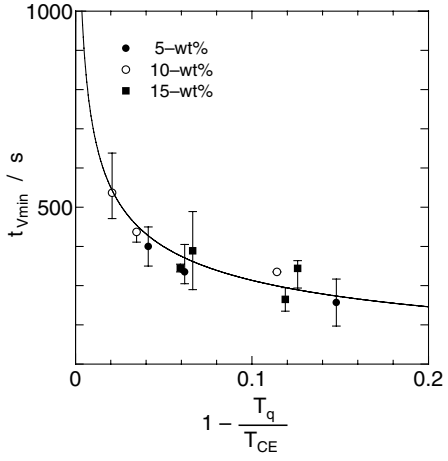

Fig. 4. The time, t_{vmin}'s obtained at different quenching temperatures are plotted against $1 - (T_q/T_{CE})$ for solutions with different concentrations.

except in a particular time interval, in which a 'mountainous' deviation was observed.

Here, the following point must be taken into account: the variation in velocity indicates that the quenching temperatures were not immediately attained after the cell was plunged into a cooling-bath, but it requires 200–300 s. That is, the experiment was carried out at not exactly equilibrium condition, but it may involve some ambiguities coming from transient effects.

The deviation from the fitted curve was found when the quenching temperature was 10°C or lower. The deviation, Δv, which is denoted by open circles, is plotted on the right hand axis against time in the same figure. The lower the quenching temperature, the larger the deviation. However, no deviation was observed when the quenching temperature was 15°C or higher. It is suggested that a critical temperature at which the deviation in velocity appears exists, and that this temperature must be between 10 and 15°C for 10 wt% iPS/*trans*-decalin solution. A similar deviation was also observed for other solutions with different concentrations: 5 and 15 wt% solutions.

It was found that the critical quenching temperature was very close to the temperature (T_{CE}) on the coexistence curve on the temperature–concentration phase diagram. The coexistence curve was numerically calculated using Flory–Shultz theory [20–22], and it is shown in Fig. 3. From the coexistence curve, the critical quenching temperatures can be estimated to be 13, 16 and 18°C for 5, 10 and 15 wt% solutions, respectively.

The time, t_{vmin} at which the deviation becomes maximum was defined; at the time, the velocity becomes minimum. As is shown in Fig. 4, the time, t_{vmin} is plotted against $1 - (T_q/T_{CE})$, where T_q is the quenching temperature. As is evident from the figure, all the t_{vmin}'s obtained at different quenching temperatures for different concentrations of solutions are put together on a curve. The time is dependent upon the quenching temperature: the time, t_{vmin} increases when the quenching temperature moved closer to the temperature on the coexistence curve (T_{CE}), while, the more the quenching temperature becomes lower than T_{CE}, the time becomes shorter. Thus, the deviation in the velocity is closely associated with liquid–liquid phase separation.

The glass transition temperature of the solutions, T_g was determined using Gordon–Taylor's equation [23], as shown in the following equation:

$$T_g^{-1} = v_p T_{gp}^{-1} + v_s T_{gs}^{-1} \tag{4}$$

where T_{gp} and T_{gs} are the glass transition temperature of iPS (100°C) and the melting temperature of *trans*-decalin (−30.4°C), respectively. v_p and v_s are the volume fractions of polymer and solvent, respectively. While, the crystallization rate is a characteristic function of temperature. Near the melting point, the rate becomes lower because of the reduction of nucleation. As the temperature is lowered, the rate increases, goes through a maximum, and then

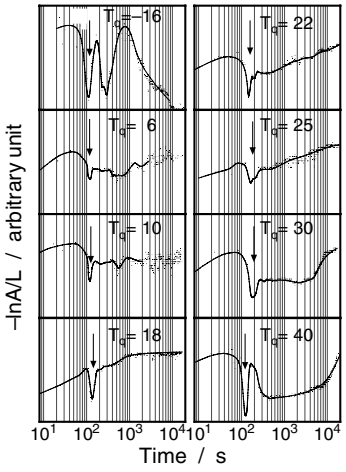

Fig. 5. The variation of $(-\ln A)/L$ with time for 10 wt% iPS/*trans*-decalin solution when the solution was allowed to quench into various temperatures (T_q). The arrow denote the time, t_{Amin}, at which $(-\ln A)/L$ becomes minimum at first.

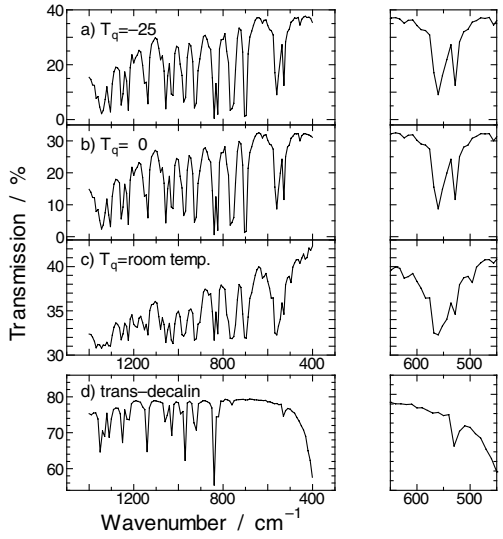

Fig. 7. The infrared absorption spectrum for iPS/*trans*-decalin gels prepared by different quenching temperatures (−25, 0°C and room temperature) and for *trans*-decalin.

decreases, as the mobility of the molecule decreases and crystallization becomes diffusion controlled. Such temperature dependence is observed for many polymers, as previously reported for natural rubber [24]. Hence, we roughly estimated the temperature giving a maximum crystallization rate as a middle point of melting point (120°C) and glass transition temperature. In Fig. 3, both the glass transition temperature (T_g) and the temperature giving the maximum crystallization rate thus obtained are shown together.

The quenching temperatures used in this study were above the glass transition temperature. Consequently, it is considered that gelation due to vitrification is ruled out. Some of the quenching temperatures were located above the coexistence curve, and others were below it. In the former case, it is suggested that no liquid–liquid phase separation occurs, but that only crystallization does. In the latter case, both the crystallization and the liquid–liquid phase separation may occur. Then, the amount of crystallization may be low and the rate of crystallization is low, since the line of T_{CE} is much lower than that of the maximum rate of crystallization as shown in Fig. 3. Accordingly, the liquid–liquid phase separation may be predominant mechanism below T_{CE}, at least at earlier times.

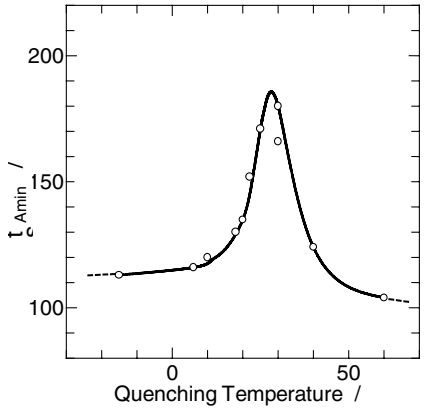

Fig. 6. The variation of t_{Amin} with quenching temperature.

Fig. 5 shows the variation of $(-\ln A)/L$) with logarithmic time when 10 wt% iPS/*trans*-decalin solution was quenched into different temperatures. As is seen in the figure, there exist a few maxima. As is indicated in Eq. (2), $(-\ln A)/L$) corresponds to the attenuation coefficient when L and A_0 are unchanged throughout the measurement. Generally, the attenuation in ultrasonic wave (i.e. $(-\ln A)/L$) will be caused by the phase transition or by the thermal relaxation [25]. Here we focus on an onset time of the second attenuation mechanism. That is, on the minimum point between the first and the second maximum, expressed by t_{Amin}, and indicated by arrows in the figure.

Fig. 6 shows the variation of t_{Amin} with the quenching temperature. The time, t_{Amin} showed a peak around 30°C for 10 wt% iPS/*trans*-decalin solution. The peak may be explained by two different kinds of mechanisms. One may be the liquid–liquid phase separation and the other the crystallization. When the quenching temperature is lower than T_{CE} the crystallization hardly occurs because of high quenching rate, but the liquid–liquid phase separation may begin to occur when the temperature goes across T_{CE} Accordingly, the liquid–liquid phase separation occurs earlier and more abundantly, as the quenching temperature becomes lower. On the other hand, when the quenching temperature is higher than T_{CE} the liquid–liquid phase separation does not occur, but the crystallization may occur. As the quenching temperature becomes higher, that is, in this case, it becomes closer to the temperature giving maximum crystallization rate, the crystallization will occur earlier and more abundantly.

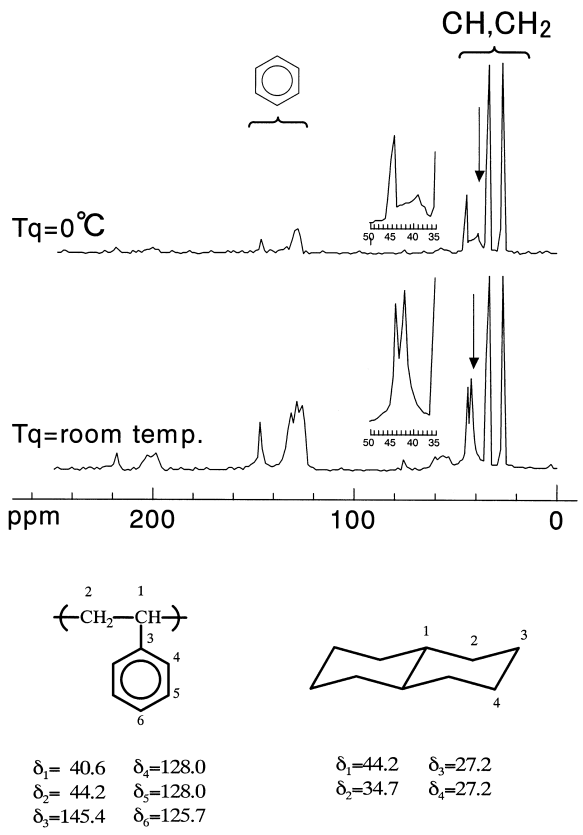

Fig. 8. The ^{13}C-CP/MAS NMR spectrum for 5 wt% iPS/*trans*-decalin gels obtained by quenching into different temperatures (0°C and room temperature). In the bottom of the figure, the assignment of the chemical shift between 30 and 50 ppm are illustrated [11,26,27].

Beside the second peak, a few peaks were observed in the figure, as described above. The first peak will give us an inkling of the change in the molecular aggregation in advance of gelation. Moreover, the third peak may be associated with the organization of crystallites. However, these points have not been clarified yet, although they are very interesting. These will be clarified in the future.

In addition, it was found that the visual and tactual nature of gels was strongly dependent on the quenching temperature. The gels prepared by quenching below T_{CE} were transparent and jelly-like to the touch. While those prepared by quenching above T_{CE} were milky and sherbet-like. Moreover, the former gels underwent a sol–gel transition at 60°C when they were heated up immediately after preparation. For the latter gels, a temperature of 120°C was required, which corresponds to the melting point of polystyrene crystallites with 3_1 helix [1]. These observations may also support that the junction point structure of gels varies with the quenching temperature.

Fig. 7 shows the infrared absorption spectra for gels prepared with different quenching temperatures: −25, 0 and room temperature (ca. 25°C). The spectrum for *trans*-decalin is shown together in the figure. Different features were observed in the wave number region between 650 and 450 cm^{-1}. For gels quenched into room temperature, the absorption bands at 624, 584 and 496 cm^{-1} were observed, but they were not observed for gels quenched into −25 and 0°C. These absorption bands are very close to the absorption bands due to TG conformation (620, 580, 566 and 500 cm^{-1}), that have been assigned by Kobayashi et al. [15]. Hence, it is concluded that the gels quenched into room temperature form the crystallites consisting of 3_1 helix, but that those quenched into −25 and 0°C do not.

Fig. 8 shows ^{13}C-CP/MAS NMR spectrum for 5 wt% iPS/*trans*-decalin gels obtained by quenching into different temperatures: 0°C and room temperature (ca. 25°C). The chemical shift observed between 30 and 50 ppm is assigned to aliphatic carbon of CH and CH_2 for solvent (*trans*-decalin) and polymer (iPS) [11,26,27], illustrated as in the bottom of the figure. A significant difference in the spectrum was found on the peak around 40 ppm, which is assigned to aliphatic carbon arising from CH of polystyrene [11,26,27]. The peak was sharp for gels obtained by quenching into room temperature (ca. 25°C), that is, a temperature above the coexistence curve. While, the peak was rather broader for gels obtained by quenching into 0°C, that is, a temperature below the coexistence curve. This peak broadening indicates the reduction of the mobility of polymer molecules, indicating a possibility of a solvated structure. Unfortunately, a concrete structure could not be given in this study. This point remains to be studied in future.

The conclusions obtained are as follows. The gelation takes place by different mechanisms, depending upon the quenching temperature. When iPS/*trans*-decalin solution is quenched above the coexistence curve, its gelation is caused by crystallization; and consequently the junction point structure is crystallite. On the other hand, when it occurs below the coexistence curve, it is caused by the liquid–liquid phase separation. Accordingly, in this case, the junction point structure must be the solvated structure consisting of polymer and solvents.

References

[1] Walter AT. J Polym Sci 1954;13:207.
[2] Gilolamo M, Keller A, Miyasaka M, Overbergh N. J Polym Sci, Polym Phys Ed 1976;14:39.
[3] Atkins EDT, Isaac MD, Keller A. J Polym Sci, Polym Phys Ed 1980;18:71.
[4] Painter PC, Kessler RE. J Polym Sci, Polym Phys Ed 1980;18:723.
[5] Atkins EDT, Keller A, Shapiro JS, Lemstra PJ. Polymer 1981;22:1161.
[6] Sundararajan PR, Tyrer NJ, Bluhm TL. Macromolecules 1982;15:286.
[7] Guenet MJ, Lotz B, Wittman JC. Macromolecules 1985;18:420.
[8] Guenet MJ. Macromolecules 1986;19:1961.
[9] Guenet MJ, McKenna GB. J Polym Sci, Polym Phys Ed 1986;24:2499.
[10] Guenet MJ. Macromolecules 1987;20:2874.
[11] Guenet MJ, McKenna GB. Macromolecules 1988;21:1752.
[12] Perez E, VanderHart DL, McKenna GB. Macromolecules 1988;21:2418.

[13] Aubert JH. Macromolecules 1988;21:3468.
[14] Klein M, Guenet MJ. Macromolecules 1989;22:3716.
[15] Kobayashi M, Nakaoki T, Ishihara N. Macromolecules 1990;23:78.
[16] Klein M, Brulet A, Guenet MJ. Macromolecules 1990;23:540.
[17] Kobayashi M, Nakaoki T. Polym Prep Jpn 1990;39:3227.
[18] Klein M, Mathis A, Manelle A, Guenet MJ. Macromolecules 1990;23:4591.
[19] Tanaka A, Nitta K, Onogi S. Polym Engng Sci 1989;29:1124.
[20] Flory PJ. J Chem Phys 1944;12:425.
[21] Shultz AR, Flory PJ. J Am Chem Soc 1952;74:4760.
[22] Flory PJ. Principles of polymer chemistry. Ithaca, NY: Cornell University Press, 1953.
[23] Gordon M, Taylor JS. J Appl Chem 1952;2:493.
[24] Wood LA. In: Mark H, Whitby GS, editors. Scientific progress in the field of rubber and synthetic elastomers, Advances in Colloid Science, vol. II. New York: Interscience, 1946.
[25] Bhatia AB. Ultrasonic absorption. New York: Oxford University Press, 1967.
[26] Bertrand RD, Moniz WB, Garroway AN, Chingas GC. J Am Chem Soc 1978;100:5227.
[27] Chingas GC, Garroway AN, Bertrand RD, Moniz WBJ. Chem Phys 1981;74:127.